JOURNAL OF GEOPHYSICAL RESEARCH, VOL. 105, NO. C12, PAGES 28,805–28,821, DECEMBER 15, 2000

Time-averaged fluxes of lead and fallout radionuclides to sediments in Florida Bay

J. A. Robbins,[1] C. Holmes,[2] R. Halley,[2] M. Bothner,[3] E. Shinn,[2] J. Graney,[4] G. Keeler,[4] M. tenBrink,[3] K. A. Orlandini,[5] and D. Rudnick[6]

Abstract. Recent, unmixed sediments from mud banks of central Florida Bay were dated using $^{210}Pb/^{226}Ra$, and chronologies were verified by comparing sediment lead temporal records with Pb/Ca ratios in annual layers of coral (*Montastrea annularis*) located on the ocean side of the Florida Keys. Dates of sediment lead peaks (1978 ± 2) accord with prior observations of a 6 year lag between the occurrence of maximum atmospheric lead in 1972 and peak coral lead in 1978. Smaller lags of 1–2 years occur between the maximum atmospheric radionuclide fallout and peaks in sediment temporal records of ^{137}Cs and Pu. Such lags are consequences of system time averaging (STA) in which atmospherically delivered particle-associated constituents accumulate and mix in a (sedimentary?) reservoir before transferring to permanent sediments and coral. STA model calculations, using time-dependent atmospheric inputs, produced optimized profiles in excellent accord with measured sediment ^{137}Cs, Pu, lead, and coral lead distributions. Derived residence times of these particle tracers (16 ± 1, 15.7 ± 0.7, 19 ± 3, and 16 ± 2 years, respectively) are comparable despite differences in sampling locations, in accumulating media, and in element loading histories and geochemical properties. For a 16 year weighted mean residence time, STA generates the observed 6 year lead peak lag. Evidently, significant levels of nondegradable, particle-associated contaminants can persist in Florida Bay for many decades following elimination of external inputs. Present results, in combination with STA model analysis of previously reported radionuclide profiles, suggest that decade-scale time averaging may occur widely in recent coastal marine sedimentary environments.

1. Introduction

Florida Bay, located at the southern end of the Florida peninsula (Figure 1), is part of an ecosystem that encompasses the southern half of the state, including the Everglades, Florida Keys, and reef tract [*Science Sub-Group*, 1995]. Recent ecological change in the Bay, including occurrences of elevated salinity, widespread sea grass mortality, eutrophication, contamination, and decline of faunal populations, have been of concern to the general public, as well as to specific interest groups, such as land managers, commercial fishermen, and recreational sportspersons. A comprehensive federal and state program was recently initiated to remedy such ecosystem deterioration [*Holloway*, 1994; *Culotta*, 1995], and an interagency group [*Drafting Committee*, 1994; *Armentano et al*., 1997] has identified research needed to address management issues. Recommended topics include a better understanding of water budgets, circulation dynamics, salinity controls, sediment buildup, nutrient cycling, and the relationship between biota and environmental changes during the past 150 years.

The ecological status of the bay during the first half of the century is known only anecdotally, with sporadic documentation available from the 1960s. Ecological assessments and salinity measurements became routine only in the 1970s. So reconstructing changes in ecosystem conditions during this century from sediment cores or other archival records is important for establishing the effects of previous human impacts and for predicting consequences of future actions. Thus a study was initiated to determine the feasibility of using the uranium series radionuclides, ^{210}Pb and ^{226}Ra, to develop appropriate sediment chronologies. Previously, *Rude and Aller* [1991] demonstrated that the method was potentially useful in Florida Bay. To validate it, sediment distributions of stable lead were compared with a time series record of lead in the banded coral *Montastrea annularis* located on the ocean side of the keys [*Shen and Boyle*, 1987]. In addition, sediment profiles of lead, as well as fallout ^{137}Cs and Pu, were compared with the time dependence of well-characterized atmospheric delivery rates. These comparisons led, in turn, to formulation and evaluation of alternative advection-diffusion and time-averaging models to account for sediment profiles.

2. Background

Sediments have been accumulating in Florida Bay for about 4000 years, following a period of wetland flooding during the last stages of Holocene sea level rise [*Scholl*, 1964a, 1964b;

[1]Great Lakes Environmental Research Laboratory, National Oceanic and Atmospheric Administration, U.S. Department of Commerce, Ann Arbor, Michigan.
[2]Center for Coastal and Regional Marine Geology, U.S. Geological Survey, St. Petersburg, Florida.
[3]Marine and Coastal Program, Woods Hole Field Center, U.S. Geological Survey, Woods Hole, Massachusetts.
[4]School of Public Health, Department of Environmental and Industrial Health, University of Michigan, Ann Arbor.
[5]Environmental Research Division, Argonne National Laboratory, Argonne, Illinois.
[6]South Florida Water Management District, West Palm Beach.

Paper number 1999JC000271.
0148-0227/00/1999JC000271$09.00

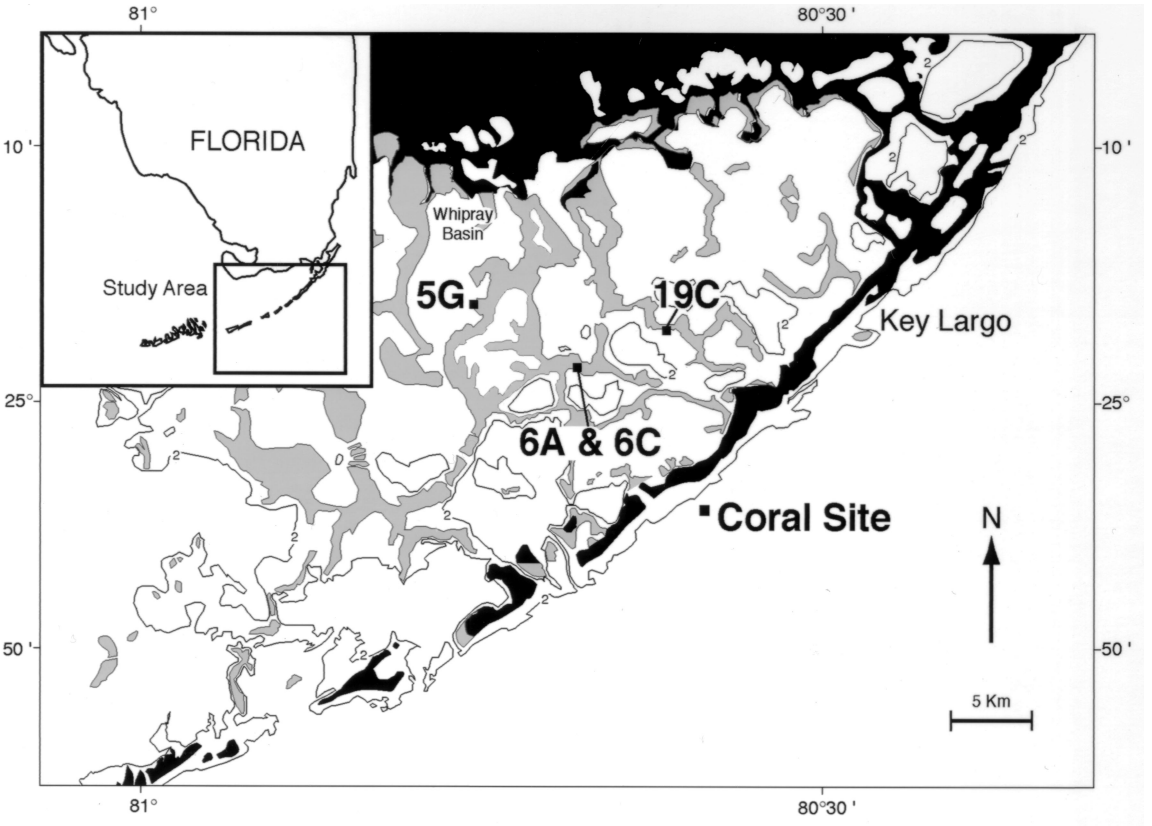

Figure 1. South Florida and the Florida Bay region. Dark areas indicate land. Cores were collected from mudbanks (shaded areas) at sites 5, 6, and 19 (dark squares) in the central region of the bay. Specimens of coral (*M. Annularis*) analyzed for lead [*Shen and Boyle*, 1987] were collected at the indicated ocean-side site (dark square).

Scholl et al., 1969; *Enos and Perkins*, 1979]. Carbon 14 dating of peats and carbonate sediments provides a general picture of the timing of sediment formation [*Enos and Perkins*, 1979; *Wanless and Tagget*, 1989]. The oldest sediments are freshwater and brackish water peats and marls, similar to those accumulating in the Everglades today [*Enos and Perkins*, 1979; *Davies and Cohen*, 1989]. These are preserved as erosion remnants on a Pleistocene limestone surface overlain by late Holocene marine sediments. Holocene sediments form a network of mudbanks and islands, partitioning the bay into more than 30 small basins, each 1–4 m deep and up to a few kilometers wide (Figure 1). Sediments are predominantly sand-, silt-, and clay-sized carbonate particles ("muds") and peats, both produced by organisms in the bay [*Ginsburg*, 1956; *Stockman et al*., 1967; *Boscence*, 1989a; *Davies and Cohen*, 1989]. Additional minor authigenic components include organic matter, opaline silica, and dolomite.

Although much is known about the origin, composition, and location of sediments in the bay [*Ginsburg*, 1956; *Stehli and Hower*, 1961; *Fleece*, 1962; *Taft and Harbaugh*, 1964; *Boscence*, 1989b], processes that redistribute them are poorly understood. *Enos and Perkins* [1979] and *Enos* [1989] have shown that many of the islands and mudbanks erode on their northern and western sides and accrete on their southern and eastern sides. *Wanless and Tagget* [1989] found layered and laminated mud to be the dominant type of sediment in mudbanks and provided evidence that layers were produced by winter cold fronts that selectively erode and redeposit fine particles. *Boscence* [1995] provides an excellent review of previous work and sedimentological history of Florida Bay mudbanks.

The preservation of layered sediments is at first surprising because the shallow bay is frequently impacted by tropical storms and hurricanes and by populations of benthic infauna. However, the intricate structure of mud banks and basins provides protected lee slopes for the accumulation of cohesive muds even in the most violent storms [*Ball et al*., 1967]. In terms of burrowing organisms, in the central part of the bay, away from the marine gulf and Atlantic boundaries, extreme variations in temperature and salinity limit their variety and abundance and high concentrations of free sulfide can severely limit the variety of organisms able to tolerate the subsurface environment [*Carlson et al*., 1994].

3. Methods

3.1. Sediment Coring

Four cores from three localities are discussed in this paper: one from Whipray Basin, two from Bob Allen Bank, and one from Russell Bank (Figure 1). These were located on southern, accretional sides of mudbanks, and cores from these areas were selected to maximize geochronological precision and accuracy. The present cores are likely not typical of most recent deposits in the bay. The core from Whipray Basin (5G) was included in this study because of its location in an area of significant ecological change during the past decade. The basin has been impacted by algal blooms and sea grass mortality,

which have characterized much of the central and western bay since the late 1980s [*Roblee et al*., 1991; *Thayer et al*., 1994]. The area has also experienced recent episodes of hypersalinity. Aerial photographs indicate that the site was largely grass-free in 1951 but subsequently developed a dense, presently impacted grass cover. Bob Allen core 6A was included to examine the influence of a long-standing grass cover on sediment radionuclide profiles. Bob Allen core 6C is from a grass-free area 16 m west of 6A, on the south slope of the bank, near the location cored by *Rude and Aller* [1991]. Russell Bank was included as a second grass-free site.

Sediment cores, 10.8 cm in diameter and up to 2 m long, were taken in May 1994 (5G, 6A, and 6C) and February 1995 (19C) using a 6 m pontoon barge, equipped with a moon pool, and piston coring equipment, based on the design of *Ginsburg and Lloyd* [1956]. Use of clear polycarbonate tubing allowed divers to observe the sediment-water interface during coring and to assure that no disturbance took place during recovery. Cores were kept in vertical position at all times, taken to local hospitals for X radiography on the evening of each collection day, and then hydraulically extruded and sectioned into 2 cm intervals using cleaned plastic utensils at a shoreside facility. Care was taken to transfer all material from each section to precleaned polyethylene bottles.

3.2. Laboratory Methods

Laboratory methods are described in detail elsewhere [*Holmes et al*., 1998]. Briefly, homogenized wet samples were placed in precleaned, preweighed porcelain evaporating dishes, dried at 40°C, cooled, and reweighed to determine water loss. Acid-insoluble content was obtained by dissolution of whole, dry sediment with 10% HCl. Portions of wet sediment were sieved through a 62 μm mesh in order to remove small amounts of shell fragments, roots, and other plant matter. Sieved sediments, dried, reground (75–100 μm), and further homogenized, were used to determine loss on ignition at 450°C. This sieved material was also used for radioisotope activity and metal concentration determinations. Activities of ^{210}Pb ($t_{1/2}$ = 22.3 years) were determined either by alpha [*Flynn*, 1968] or gamma [*Cutshall et al*., 1983] spectroscopy. Activities of ^{137}Cs ($t_{1/2}$ = 30.2 years) and ^{226}Ra ($t_{1/2}$ = 1600 years) were determined by gamma spectroscopy, with the radium determination based on in-growth of radon decay products in suitably aged sealed samples. The unresolved isotopes of plutonium $^{239+240}$Pu ($t_{1/2}$ = 24 and 6.6 kyr, respectively) and ^{241}Am ($t_{1/2}$ = 458 years) were determined following methods described by *Kaplan et al*. [1994]. Lead concentrations were determined by analysis of ultrapure nitric acid extracts of sediments using an inductively coupled plasma-mass spectrometry (ICP-MS) system [*Graney et al*., 1995]. All activity and concentration determinations were standardized using National Institute of Standards and Technology (NIST) standards.

3.3. Historical Inputs of ^{137}Cs, Pu, and Pb to the Florida Bay Region

Rates of deposition of ^{137}Cs were based on monthly measurements of ^{90}Sr fallout as determined at the University of Miami School of Medicine in Coral Gables, Florida, from April 1957 through June 1971, and at the U.S. Weather Bureau Airport Station in Miami from February 1963 through June 1976 [*Health and Safety Laboratory* (*HASL*), 1977]. Missing data were supplied by linear scaling of a complete fallout record for the U.S. midwestern region [*HASL*, 1977] to the Miami records. Rates of ^{137}Cs deposition (Figure 2a) were calculated as 1.66 times values of ^{90}Sr [*Robbins*, 1985]. Rates of Pu (=$^{239+240}$Pu) deposition were calculated as 0.016 and 0.012 times ^{137}Cs deposition rates, based on premoratorium and postmoratorium (1960) production ratios, respectively [*Koide et al*., 1982].

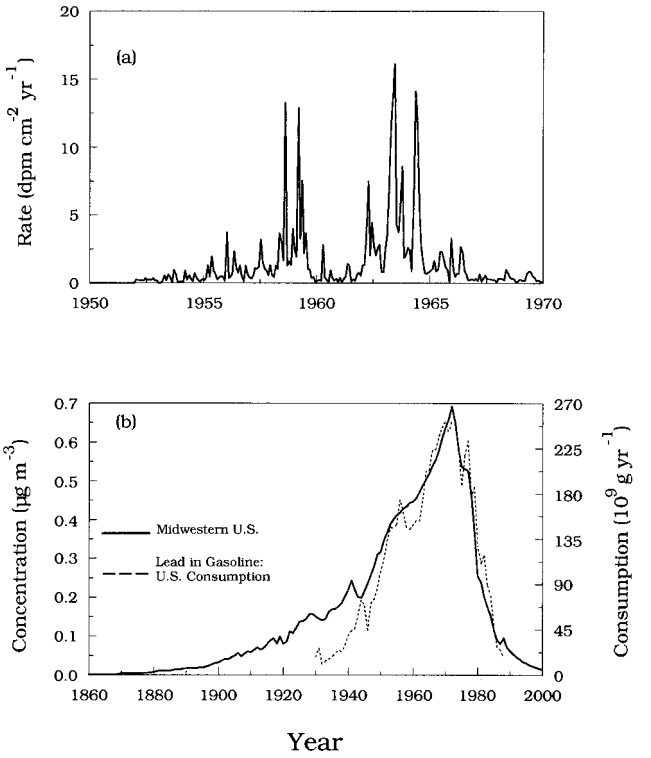

Figure 2. (a) Record of ^{137}Cs deposition at Miami. This function has been used to calculate model profiles of ^{137}Cs in cores. (b) Generalized record of nonurban atmospheric lead concentrations based on historical reconstruction and atmospheric measurements in the Great Lakes region (solid line). This source function is used to calculate model profiles of lead in sediments and coral. The dashed line shows the U.S. annual consumption of lead in gasoline between 1930 and 1988.

Because a well-developed history of atmospheric lead deposition was not available for the south Florida area, this study used historical records of atmospheric Pb concentrations as reported by *Eisenreich et al*. [1986] and extended to the early 1990s by *Graney et al*. [1995]. This record (Figure 2b) is used to represent the relative time dependence (but not the magnitude) of nonurban atmospheric lead deposition in the eastern continental United States, including Florida Bay. Between 1950 and 1990, when combustion of leaded fuels was the dominant source of atmospheric lead, this record tracks closely with gasoline lead consumption in the United States as reported by *Nriagu* [1990] and *Wu and Boyle* [1997].

4. Results and Discussion

4.1. Stratigraphy of Sediment Cores

Stratigraphic differences between cores collected from grass-covered sites (Whipray 5G and Bob Allen 6A) and those from barren areas (Bob Allen 6c and Russell Bank 19C) are apparent in Figure 3. Both 5G and 6A show considerable

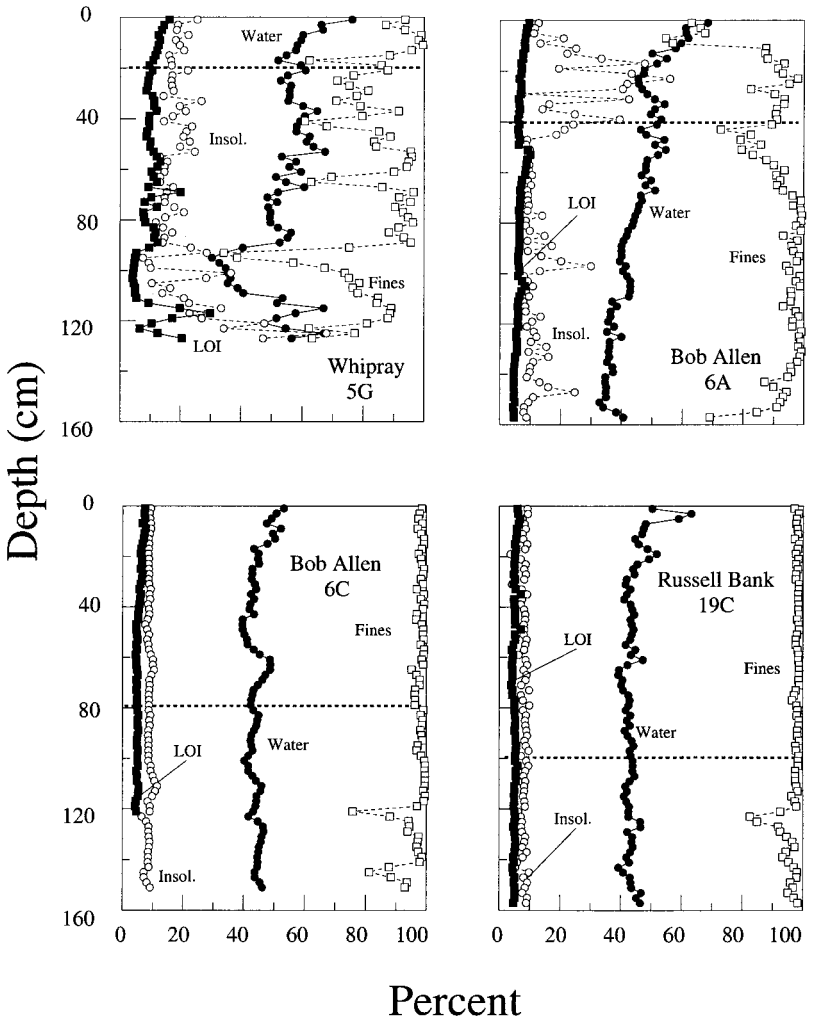

Figure 3. Composition of major constituents in four cores (percent water and percent fines <62 μm = 100xg/g whole dry sediment; percent insoluble and loss-on-ignition = 100xg/g fines). Sites 5G (Whipray Basin) and 6A (Bob Allen Bank) are densely covered with turtle grass (*Thelassia testudinum*) having roots penetrating to ~30 cm. Sites 6C (Bob Allen Bank) and 19C (Russell Bank) are grass-free and evidence considerably less stratigraphic variability. Excess ^{210}Pb occurs in core sections above the indicated horizontal (dashed) lines.

downcore variability in the amount of fine sediment, the amount of acid-insoluble residue (noncarbonate minerals and organic material), and the loss on ignition of primarily organic components from sieved sediments. Since 6A and 6C are less than 20 m apart, stratigraphic differences between them likely arise from the presence and action of grasses and grass-associated fauna. The thickness of sediment relevant for the present study (i.e., having significant excess ^{210}Pb, as indicated by horizontal dashed lines in Figure 3) varies significantly among sites: above about 20, 40, 80, and 100 cm at 5G, 6A, 6C, and 19C, respectively. In core 5G sections above 20 cm, means ($\pm$ standard deviation) of percent fines (100x g fine/g whole dry), and insoluble and loss on ignition (g insoluble or g lost/g fines) are 90 $\pm$ 11, 20 $\pm$ 3, and 12 $\pm$ 2, respectively. Coefficients of variation (CV = 100 (standard deviation/mean)) are only about 10%. In core 6A above 70 cm the values are 85 $\pm$ 11, 21 $\pm$ 14, and 7 $\pm$ 1, respectively. Considerable variability (CV = 66%) in the insoluble fraction is due to large, fluctuating amounts of grass stems and roots that penetrated down to about 30 cm that were removed by sieving. In cores 6C and 19C from grass-free sites the corresponding values are 98 $\pm$ 1, 9 $\pm$ 1, and 5.5 $\pm$ 0.9 above 80 cm and 99 $\pm$ 1, 8 $\pm$ 1, and 5.1 $\pm$ 0.7 above 100 cm, respectively. In these cores, X radiographs of sections above these respective depths reveal numerous millimeter to submillimeter thick, faintly contrasting horizontal bands with no other significant stratigraphic features [*Holmes et al*., 1998]. The X radiograph of core 19C indicated a particularly long uniform sequence of layered, undisturbed sediment.

4.2. Lead 210/Radium 226 Chronology

The ^{210}Pb method [*Goldberg*, 1963] exploits occurrences of disequilibrium between ^{226}Ra and its long-lived decay product ^{210}Pb. *Robbins* [1978], *Appleby and Oldfield* [1992], and *Robbins and Herche* [1993] have reviewed various measurement techniques, applications, and approaches to modeling ^{210}Pb. The method has been widely used in coastal marine environments to obtain rates of sediment accumulation, as well as depths and rates of mixing of near-surface sediments.

In the Florida Bay cores, total ^{210}Pb is significantly higher than ^{226}Ra in near-surface sediments and approaches secular

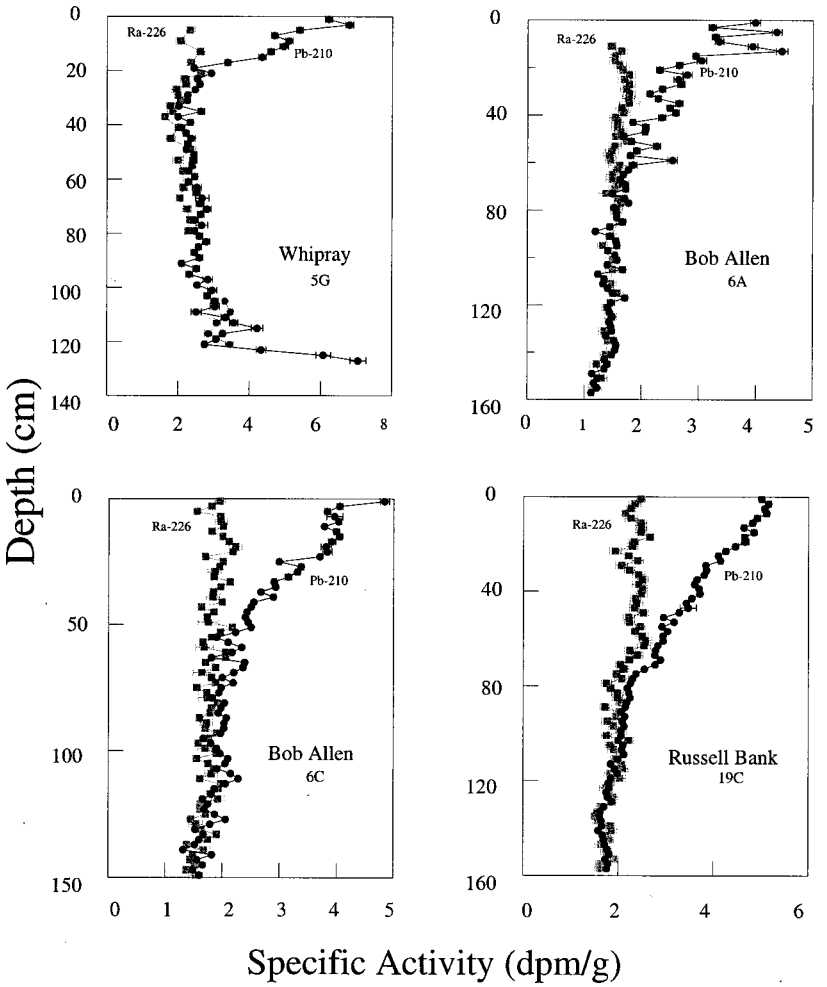

Figure 4. Total ^{210}Pb (solid circles) and ^{226}Ra (shaded squares). ^{210}Pb activities exceed ^{226}Ra (by $\sim 2x$) in near-surface sediments and approach secular equilibrium with increasing depth. The major increase in ^{210}Pb activity near the bottom of core 5G occurs within a basal peat layer contacting porous Pleistocene limestone through which ^{226}Ra presumably migrates upward.

equilibrium with depth (Figure 4). In core 5G, total ^{210}Pb and ^{226}Ra are essentially in secular equilibrium below about 25 cm. Below about 40 cm, activities of both nuclides gradually increase with depth. The pronounced upward excursion in total ^{210}Pb activity in the bottom 8 cm of this core occurs within basal peat in contact with porous Pleistocene limestone bedrock through which presumably radium-rich interstitial waters may migrate (J. Chanton and W. Burnett, personal communication, 1998). Distributions of radium in the other three cores (6A, 6C, and 19C) decrease with increasing depth in accord with earlier observations by *Rude and Aller* [1991], with about a 20% difference in mean activity between sites. In core 6A, large fluctuations in total ^{210}Pb activities occur in the upper 15 cm, where roots and plant fragments are abundant (Figure 3), but activities do not correlate significantly with principal stratigraphic variables.

Sediment chronologies are based on constant net rates of supply of excess ^{210}Pb, F_o (disintegrations per minute (dpm) cm^{-2} yr^{-1}), and mass, r_s (g cm^{-2} yr^{-1}). Excess ^{210}Pb activity (dpm g^{-1}), defined as the difference between total ^{210}Pb and ^{226}Ra, is calculated as,

$$A_{ex}(g) = \frac{F_o}{r_s} e^{-\lambda g/r_s}, \quad (1)$$

where g (g cm^{-2}) is the cumulative weight of sediment at a given depth and λ is the radioactive decay constant ($\ln 2/t_{1/2} = 0.03114$ yr^{-1}). Equation (1), which automatically takes account of sediment compaction, implicitly assumes no postdepositional radionuclide mobility or sediment mixing. Least squares–optimized values of r_s and surface activity of excess ^{210}Pb, $A_{ex}(0) = F_o/r_s$, are provided in Table 1. Sediment ages (years B.P.) are calculated as g/r_s. Excess ^{210}Pb data are plotted versus cumulative sediment weight in Figure 5 to illustrate the generally excellent agreement between observed excess ^{210}Pb profiles and the above simple exponential model. Note that neither core 6A nor 6C had a zone of essentially constant ^{210}Pb activity such as that reported by *Rude and Aller* [1991] in their core from Bob Allen Bank.

Age-depth relations based on mass accumulation rates (equation (1)) are shown with envelopes of uncertainty (± 2 standard deviations) in Figure 6 (solid line enclosed by dotted lines). For core 5G, time assignments are extrapolations before

Table 1. Summary of Uranium Series Nuclide Analytical Data and Chronological Model Parameters

Quantity[a]	Wipray Core 5G	Bob Allen Core 6A	Bob Allen Core 6C	Russell Bank Core 19C
Mean ^{238}U,[b] dpm g^{-1}	—	2.4 ± 0.5	2.4 ± 0.3	2.5 ± 0.3
Mean ^{226}Ra,[b] dpm g^{-1}	2.0 ± 0.4	1.7 ± 0.4	1.8 ± 0.4	2.1 ± 0.3
Excess ^{210}Pb Inventory, dpm cm^{-2}	24 ± 3	40 ± 3	73 ± 3	98 ± 4
Surface Excess ^{210}Pb,[c] dpm g^{-1}	4.3 ± 0.1	2.39 ± 0.06	2.65 ± 0.04	3.13 ± 0.04
Mass Accumulation Rate,[c] g cm^{-2} yr^{-1}	0.17 ± 0.01	0.51 ± 0.02	0.79 ± 0.02	0.92 ± 0.02
Fit Standard Deviation, dpm g^{-1}	0.478	0.474	0.259	0.238

[a]Mass units are in grams of whole dry sediment.
[b]Average of all values.
[c]Standard deviations are based on Marquardt-Levenberg nonlinear parameter estimation [*Press et al.*, 1989].

1925; for the rest, they are extrapolations before 1900. In core 5G, 2 cm core sections span time intervals ranging from 3 years at the surface to 7 years at a depth corresponding to 1900. In the other cores, times range from about 1 year at the surface to 2–3 years in 1900. This time characterizes the maximum resolution with which events can be reconstructed under the experimental conditions.

4.3. Lead in Dated Sediments and Coral

Temporal records of lead in sediment cores 6A, 6C, and 19C and in layers of annually banded coral, *M. annularis* [*Shen and Boyle*, 1987] located on the ocean side of Plantation Key about 1.5 km offshore (Figure 1), are compared in Figure 7. Sediment lead records (solid circles) are consistent among sites,

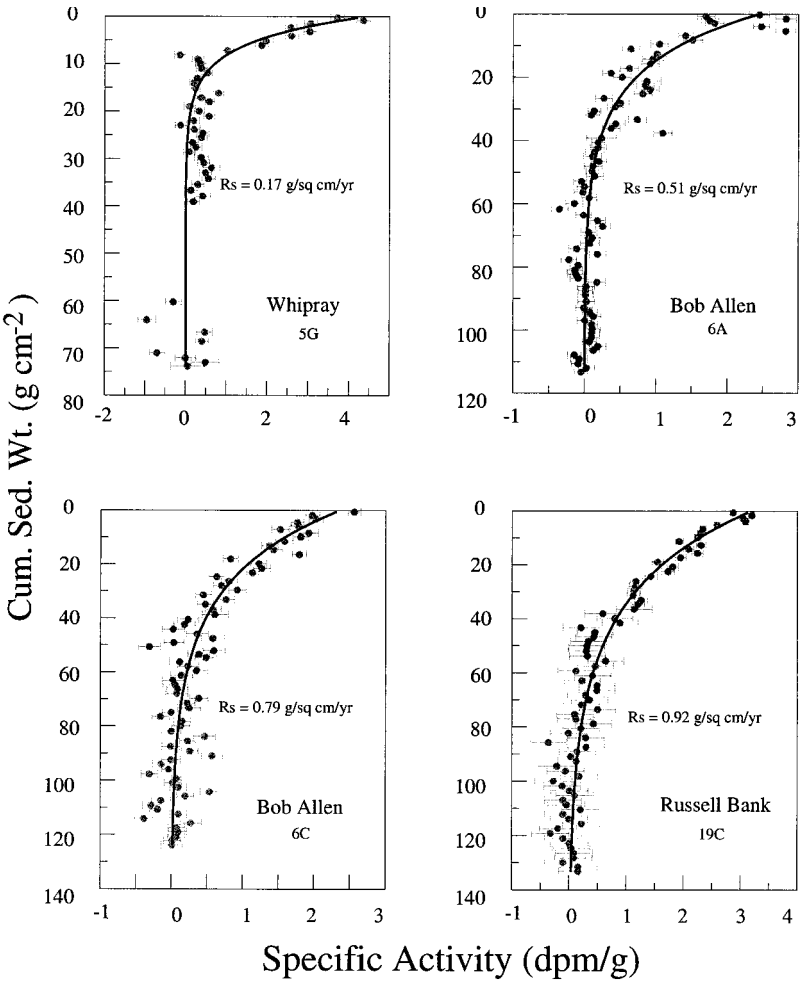

Figure 5. Excess ^{210}Pb versus cumulative dry weight of sediment. Exponential model profiles are shown as solid lines. Mean accumulation rates vary more than fivefold among cores and are determined with greatest precision in two cores from grass-free sites (6C and 19C).

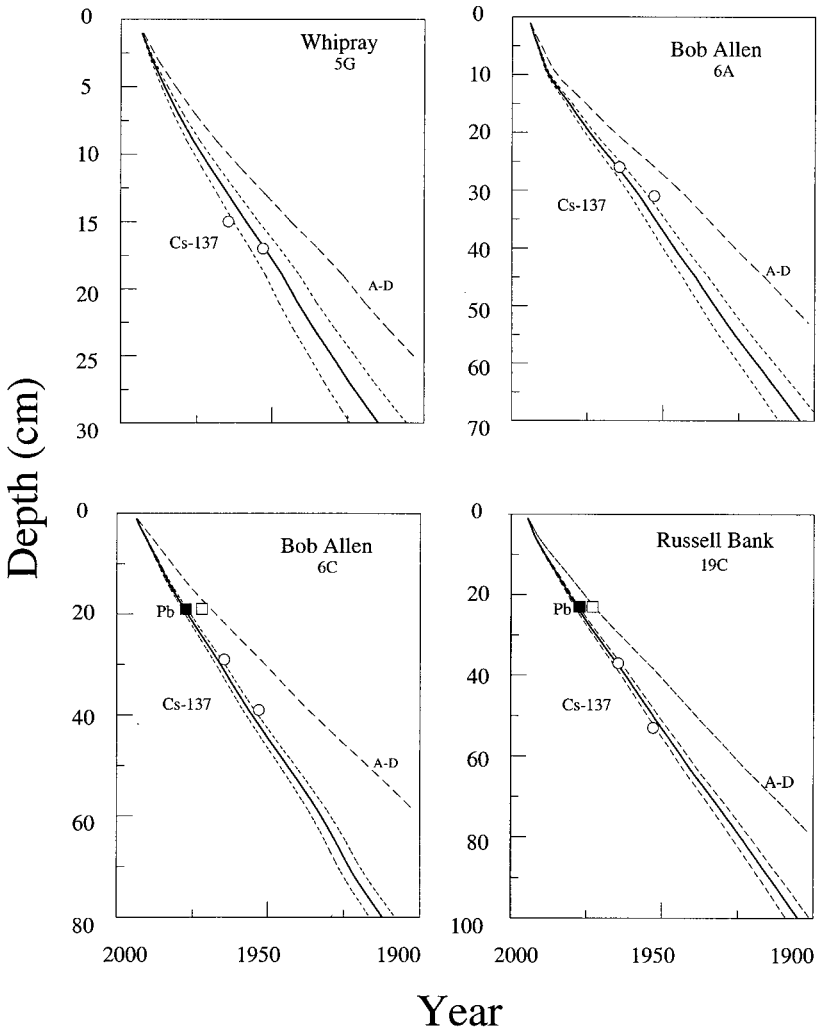

Figure 6. Age-depth relations (with uncertainty envelopes of ±2 standard deviations) based on ^{210}Pb. Assignments of dates (1964 and 1952) to depths of ^{137}Cs profile peaks and penetration depths agree with ^{210}Pb dates (open circles). These assignments are incompatible with A-D model dates (dashed lines). Assignment of 1978 (coral lead peak) to lead peaks in cores 6C and 19C accords with ^{210}Pb dates (dark square); assignment of 1972 (continental atmospheric lead peak) does not (open squares).

although the near-surface record is incomplete for core 6A. Backgrounds are comparable at each site, averaging 1.6 ± 0.1 μg g^{-1}. Excess lead concentrations (total minus background), as for excess ^{210}Pb, are not much ($<2x$) greater than background levels. In coral layers, Pb/Ca ratios (open squares) are in excellent accord with the sediment records. In cores 6C and 19C, lead maxima occur at 1978 ± 2 years (Table 2), in accord with the prior observation of a 6 year lag between peak atmospheric lead in 1972 and maximum coral lead [*Shen and Boyle*, 1987]. Also excess Pb/excess ^{210}Pb ratios are comparable in coral and sediment samples of the same age. In 1982 (coral sample collection year), excess Pb was about 24 nmol Pb/mol Ca = 124 ng Pb/g Ca or about 0.049 μg Pb/g coral assuming coral is essentially 100% $CaCO_3$. Decay-corrected excess ^{210}Pb was 0.15 dpm/g coral [*Shen and Boyle*, 1988]. Thus excess Pb/excess ^{210}Pb = 0.049/0.15 = 0.33 μg dpm^{-1}. In cores 6A, 6C, and 19C the average ratio in 1982 was 0.37 ± 0.09 μg dpm^{-1}. This ratio is also consistent with Pb/^{210}Pb ratios (see section 4.6) in rain collected at Pigeon Key in 1978 [*Settle et al.*, 1982].

These observations suggest that the atmosphere is the primary source of lead species (both Pb and ^{210}Pb) that are delivered to sediments and coral (receptors). Evidently, both receptors accumulate lead species in proportion to their concentrations in ambient waters despite differences in principal modes of incorporation, i.e., particle scavenging versus coral lattice-binding of dissolved Pb [*Shen and Boyle*, 1988]. Also, if receptors reside in largely nonexchanging water masses (e.g., Florida Bay versus Florida Straits), temporal lead records must, nevertheless, be comparably transformed over time to accord with present observations. Finally, the excellent agreement between sediment and coral Pb records confirms the ^{210}Pb chronology.

4.4. Distributions of ^{137}Cs, Pu, and ^{241}Am

Significant deposition of ^{137}Cs commenced following aboveground testing of nuclear weapons in 1952 [*Carter and Moghissi*, 1977] and reached maxima of nearly equal intensity at Miami in June of 1963 and May of 1964 (Figure 2a). Much of the structure evident in this temporal record is lost in cor-

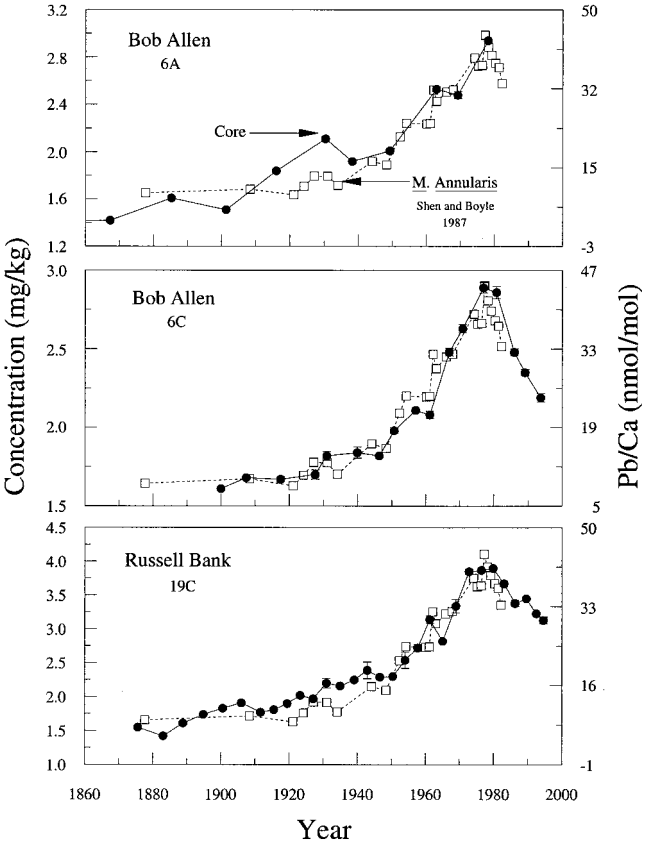

Figure 7. Concentrations of lead in cores 6A, 6C, and 19C (solid circles) versus ^{210}Pb dates. Molar ratios of Pb/Ca in annual layers of *M. Annularis* are superimposed (open squares) using coral layer ages. The agreement demonstrates the validity of ^{210}Pb/^{226}Ra dating. Evidently, sediments and coral have been exposed to and recorded essentially the same changes in ambient lead concentrations in water during the past century.

responding sediment profiles (Figure 8). Obviously, a small part of this loss could be due to time averaging 1–2 years of record by sectioning cores in 2 cm intervals. Activities generally increase from low but detectable levels in surface sediments to broad maxima, located at depths ranging from 15 to about 40 cm (Table 3 and Figure 8, lightly shaded horizontal line segments). The depth of penetration of ^{137}Cs (similarly indicated in Figure 8) is calculated as the location of the top of the first core section, which has no significant radiocesium activity ($>2\sigma$), proceeding downcore from the surface. Correspondences between ^{137}Cs peak and penetration depths and years of maximum fallout (1964) and onset (1952) accord very well with mean ($\pm$ standard error) dates for the four cores based on ^{210}Pb age-depth relations (Figure 6, open circles, and Table 3): 1965 $\pm$ 1 and 1953 $\pm$ 1 years, respectively.

Distributions of Pu and ^{241}Am in core 19C (Table 4) are also consistent with dates of onset and maximum fallout. Maxima occur in the 34–40 cm interval corresponding to a mean ^{210}Pb date of 1965 $\pm$ 3 years. The deepest interval having detectable levels of these nuclides was 48–54 cm with a ^{210}Pb date of 1952 $\pm$ 3 years (where "errors" reported reflect the half-width of composite intervals). The ^{241}Am/Pu ratio is essentially constant downcore, 0.40 $\pm$ 0.02, and approaches the theoretical maximum ratio of 0.42 that is expected in the year 2037 [*Krey et al*., 1976; *Koide et al*., 1980].

4.5. Postdepositional Radionuclide Mobility?

Peak and penetration depths of ^{137}Cs and Pu occur at correct dates within experimental error in all cases, thus further confirming ^{210}Pb chronologies and indicating insignificant postdepositional mobility. This is at first surprising since numerous studies have suggested that ^{137}Cs may be mobile in marine sediments [*Santschi et al*., 1983; *Sholkovitz*, 1983; *Sholkovitz et al*., 1983; *Sholkovitz and Mann*, 1984; *Olsen et al*., 1981]. These observations notwithstanding, radionuclide distributions in the Florida Bay cores cannot be consistently interpreted in terms of diffusive migration using a conventional, non–steady state advection-diffusion (A-D) model [*Berner*, 1980; *Robbins*, 1986] employing the local equilibrium approximation [*Bahr and Rubin*, 1987] with reversible tracer exchange between pore water and solids.

A-D model fits to ^{137}Cs profiles, yielding optimized distribution coefficients (K_ds), may seem to be in reasonable accord with observed profiles (Figure 8) on a case-by-case basis. However, derived mass accumulation rates (Table 3) seriously conflict with those from ^{210}Pb (Table 1 and age-depth relations

Table 2. Summary of Analytical Data and STA Model Parameter Values for Pb[a]

Quantity	Bob Allen Core 6A	Bob Allen Core 6C	Russell Bank Core 19C
Background Concentration,[b] μg g^{-1}	1.6 $\pm$ 0.1	1.6 $\pm$ 0.1	1.6 $\pm$ 0.1
Maximum Concentration, μg g^{-1}	2.9 $\pm$ 0.1	2.9 $\pm$ 0.1	3.9 $\pm$ 0.2
Peak Depth,[c] cm	$<$17 $\pm$ 2	19 $\pm$ 2	25 $\pm$ 4
Peak Year[d]	$>$1978 $\pm$ 3	1979 $\pm$ 2	1976 $\pm$ 3
Mass Accumulation Rate,[e] g cm^{-2} yr^{-1}	$<$0.78 $\pm$ 0.03	0.77 $\pm$ 0.08	0.86 $\pm$ 0.04
STA Model Residence Time,[f] year	15 $\pm$ 6[g]	16 $\pm$ 2	22 $\pm$ 2

[a]Reported uncertainties are standard deviations unless noted otherwise.
[b]Approximate uncertainty in assignment of background Pb concentrations.
[c]Standard deviations estimated by inclusion of all intervals around the peak value with concentrations not significantly different from the maximum.
[d]Based on ^{210}Pb dates. Dates are assigned to 6A on the assumption that missing concentration values above 10 cm depth would be lower than the maximum at 17 cm.
[e]Rates calculated by optimizing the overlap with the coral Pb record. Standard deviations calculated by Monte Carlo methods assuming an overall 3% error in determination of coral and sediment Pb concentrations.
[f]Values calculated with accumulation rates based on ^{210}Pb. Standard deviations were determined by Monte Carlo methods.
[g]The larger error in this value reflecting its greater sensitivity to uncertainty in the ^{210}Pb accumulation rate because of missing near-surface ^{210}Pb data.

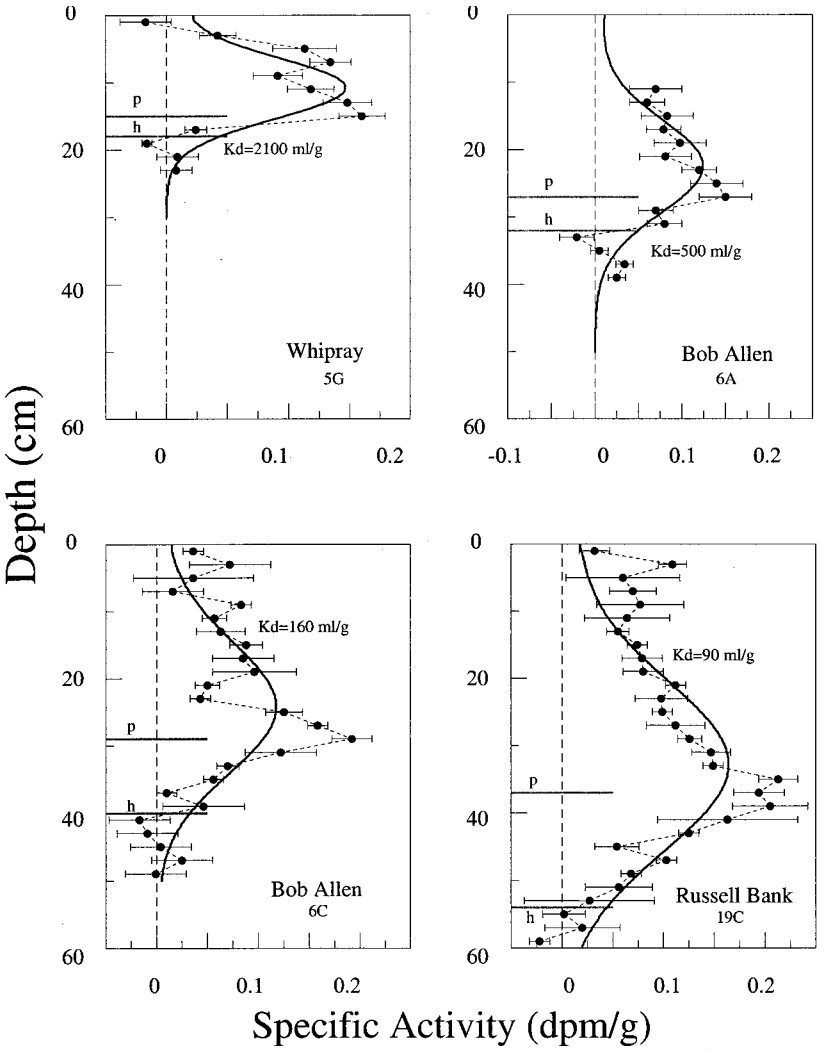

Figure 8. Profiles of ^{137}Cs. The horizontal line segments indicate positions of peak activities (p) and penetration depths (h). The depth scale is the same in each panel to emphasize effects of differences in sediment accumulation rates among sites. Calculated advection-diffusion (A-D) model profiles agree reasonably with observations taken separately. However, incompatibilities in distribution coefficients (K_d) and sediment accumulation rates with other data (see text) are artifacts of using an inappropriate diagenetic (A-D) model in cases where sedimentary ^{137}Cs is particle-bound.

and Figure 6, dashed line). Calculated distribution coefficients decrease systematically (Table 3) by a factor of more than 20 from the core with the lowest mass accumulation rate (Whipray 5G, K_d = 2100 mL g^{-1}) to that with the highest rate (Russell Bank 19C, K_d = 90 ± 10 mL g^{-1}). This trend is unreasonable because significant differences in geochemical environments between cores, which could realize such large changes in distribution coefficients, are unlikely. Finally, theoretical activities of ^{137}Cs penetrate significantly deeper into sediments than those observed in the cores. Evidently, these several faults result from use of a model that incorrectly attributes radiocesium profile shapes largely to postdepositional mobility. Present results are consistent with a 10 year time series of ^{137}Cs profiles in ^{210}Pb-dated illitic sediment cores from Skan Bay, Alaska, in which there was negligible mobility of the radionuclide [*Sugai et al*., 1994]. It should be noted that small amounts of radiocesium-binding illite [*Comans and Hockley*, 1992] occur in sediments of central Florida Bay [*Manker and Griffin*, 1971].

4.6. Atmospheric Delivery Rates, Sediment Inventories, and Focusing Factors

The average atmospheric flux of ^{210}Pb in the Florida Bay region has been estimated by *Settle et al*. [1982] as about 0.43 dpm cm^{-2} yr^{-1}. This value, based on measurement of ^{210}Pb in rain samples collected on Pigeon Key (Figure 1) during 1978, is probably too low because it does not include contributions from dry deposition. In 1997 the mean total (wet plus dry) deposition rate of ^{210}Pb in the Miami area was 0.7 dpm cm^{-2} yr^{-1} (D. Kadko, personal communication, 1998). This value is more in accord with atmospheric deposition rates in coastal areas at Norfolk, Virginia; New Haven, Connecticut; and Long Island, New York; selected from data summarized by *Urban et al*. [1990], average 0.9 ± 0.2 dpm cm^{-2} yr^{-1}. This latter value corresponds to a cumulative excess ^{210}Pb load (standing crop) of about 30 dpm cm^{-2}. Thus values of vertically integrated excess ^{210}Pb in sediments, inventories of 24 ± 3, 40 ± 3, 73 ± 3, and 98 ± 4 dpm cm^{-2} (mean ± standard deviation, 60 ± 30;

Table 3. Mean Mass Accumulation Rates and Other Model Parameters Derived From ^{137}Cs Profiles

Quantity	Whipray Core 5G	Bob Allen Core 6A	Bob Allen Core 6C	Russell Bank Core 19C
Values From Time Assignments to Profile Features				
Peak depth,[a] cm	15 ± 1	27 ± 1	29 ± 1	35 ± 1
Mass Accumulation Rate from peak,[b] g cm^{-2} yr^{-1}	0.20 ± 0.01	0.53 ± 0.04	0.73 ± 0.03	0.85 ± 0.02
Horizon Depth, cm	18 ± 1	32 ± 1	40 ± 1	58 ± 1
Mass Accumulation Rate from horizon,[c] g cm^{-2} yr^{-1}	0.18 ± 0.01	0.46 ± 0.02	0.73 ± 0.03	1.06 ± 0.02
Advection-Diffusion (A-D) Model Values[d]				
Mass Accumulation Rate, g cm^{-2} yr^{-1}	0.12 ± 0.01	0.36 ± 0.03	0.52 ± 0.03	0.69 ± 0.03
Distribution Coefficient, mL g^{-1}	2100 ± 400	500 ± 100	160 ± 30	90 ± 10
Fit Standard Deviation, dpm g^{-1}	0.037	0.029	0.035	0.034
System Time Averaging (STA) Model Values[d]				
Mass Accumulation Rate, g cm^{-2} yr^{-1}	0.20 ± 0.02	0.54 ± 0.03	0.78 ± 0.02	1.06 ± 0.04
Residence Time, years	16 ± 2	16 ± 4	14 ± 2	17 ± 3
Fit Standard Deviation, dpm g^{-1}	0.031	0.019	0.026	0.021

[a]Standard deviations approximated as half the sectioning interval size.
[b]Based on assigning the year 1964 to depth of ^{137}Cs maximum expressed as a cumulative sediment weight (g cm^{-2}) in each core.
[c]Based on assigning the year 1952 to the deepest interval (cumulative sediment weight) having ^{137}Cs activity significantly above background (horizon).
[d]Based on Monte Carlo methods [*Press et al*., 1989].

CV, 50%), correspond to focusing factors (excess ^{210}Pb inventory/standing crop) of 0.8, 1.3, 2.4, and 3.3 (dpm cm^{-2} sediment/dpm cm^{-2} system) at sites 5G, 6A, 6C, and 19C, respectively (Table 5). Thus inventories are comparable to or do not greatly exceed amounts expected from atmospheric deposition alone.

Excess Pb inventories are 29 ± 3, 38 ± 3, and 80 ± 5 μg cm^{-2} (mean ± standard deviation, 49 ± 30; CV, 60%) at sites 6A, 6C, and 19C, respectively (Table 5). Ratios of excess Pb to excess ^{210}Pb inventories in respective cores are 0.73 ± 0.09, 0.52 ± 0.06, and 0.82 ± 0.06 μg dpm^{-1} (mean ± standard deviation, 0.69 ± 0.15; CV, 20%) and are comparatively constant among sites. This ratio may be used to estimate the average cumulative loading of excess Pb to the bay as 0.69 μg dpm^{-1} × 30 dpm cm^{-2} = 20 μg cm^{-2} as of 1995. From this value, focusing factors for excess lead in 6A, 6C, and 19C are 1.5, 1.9, and 4.0 (μg cm^{-2} sediment/μg cm^{-2} system), respectively, and are comparable to those for excess ^{210}Pb. This method of estimating cumulative Pb loading is appropriate if ^{210}Pb and Pb have had comparable modes of delivery to the bay (i.e., primarily atmospheric) and have been subject to similar processes of transport and accumulation in sediments over time.

That the atmosphere is the main source of excess Pb to the bay is suggested by the compatibility of the mean Pb/^{210}Pb sediment inventory ratio 0.69 μg dpm^{-1} with ratios in rainfall, as determined by *Settle et al*. [1982]. Their reported ratios varied between 0.25 and 0.90 (μg dpm^{-1}), depending on whether atmospheric conditions favored marine or continental sources, respectively. The sediment core Pb data may be used more precisely to estimate a mean annual rate of excess lead loading to the Florida Bay system in 1978, the year with maximum sediment Pb concentrations. In cores 6A, 6C, and 19C maximum excess Pb concentrations are 1.3, 1.3, and 2.3 μg g^{-1}, respectively, and correspond to excess Pb sediment fluxes of 0.80, 1.0, and 2.1 μg cm^{-2} yr^{-1}. After dividing these values by focusing factors of 1.5, 1.9, and 4.0, as determined above, rates of Pb loading to the system in 1978 were 0.53, 0.55, and 0.52 μg cm^{-2} yr^{-1} for cores at 6A, 6C, and 19C, respectively. Using a ^{210}Pb atmospheric delivery rate of 0.9 dpm cm^{-2} yr^{-1} and the above range in Pb/^{210}Pb concentration ratios in rainfall, Pb deposition at Pigeon Key is estimated to have varied from

Table 4. Activities of ^{137}Cs, $^{239+240}$Pu, and ^{241}Am in Whole Composite Sediment Samples From Russell Bank (19C)

Range, cm	Mean, cm	Year[a]	Pu, dpm kg^{-1}	Am, dpm kg^{-1}	^{137}Cs,[b] dpm kg^{-1}	Am/Pu	Cs/Pu
2–12	7	1991	25 ± 2	11 ± 1	90 ± 20	0.43 ± 0.05	3.4 ± 0.6
12–18	15	1985	32 ± 2	13 ± 1	90 ± 10	0.41 ± 0.04	2.7 ± 0.4
18–24	21	1980	31 ± 2	12 ± 1	140 ± 16	0.39 ± 0.04	4.5 ± 0.6
26–32	29	1973	39 ± 2	16 ± 1	210 ± 20	0.42 ± 0.04	5.5 ± 0.6
34–40	37	1965	74 ± 4	29 ± 2	410 ± 20	0.40 ± 0.03	5.6 ± 0.4
42–48	45	1958	37 ± 2	25 ± 1	229 ± 20	0.40 ± 0.04	6.0 ± 0.7
48–54	51	1952	13 ± 1	2.3 ± 0.3	130 ± 70	0.40 ± 0.06	11 ± 5
60–70	65	1940	0.12 ± 0.09	—	0 ± 50	—	—

[a]Date assignments are based on (2).
[b]The activity of ^{137}Cs is corrected for postdepositional decay.

Table 5. Excess ^{210}Pb, ^{137}Cs, and Net Pb Inventories, Ratios, and Relations to Estimated Atmospheric Loads to the Florida Bay Region

	Whipray Core 5G	Bob Allen Core 6A	Bob Allen Core 6C	Russell Bank Core 19C
Mean Sediment Accumulation Rate,[a] g cm^{-2} yr^{-1}	0.17 ± 0.01	0.51 ± 0.02	0.79 ± 0.02	0.92 ± 0.02
Inventories				
Excess ^{210}Pb, dpm cm^{-2}	24 ± 3	40 ± 3	73 ± 3	98 ± 4
^{137}Cs, dpm cm^{-2}	0.75 ± 0.05	1.8 ± 0.2	2.4 ± 0.2	4.5 ± 0.3
Net Pb, μg cm^{-2}	—	29 ± 3	38 ± 4	80 ± 5
$^{239+240}$Pu	—	—	—	1.6 ± 0.1
Inventory Ratios				
^{137}Cs/Excess ^{210}Pb	0.031 ± 0.004	0.045 ± 0.006	0.033 ± 0.003	0.046 ± 0.004
Net Pb/Excess ^{210}Pb, μg dpm^{-1}	—	0.73 ± 0.09	0.52 ± 0.06	0.82 ± 0.06
^{137}Cs/Net Pb, dpm μg^{-1}	—	0.062 ± 0.009	0.063 ± 0.009	0.056 ± 0.005
^{137}Cs/$^{239+240}$Pu	—	—	—	2.8 ± 0.3
Inventories Relative to Atmospheric Loads[b]				
Excess ^{210}Pb	0.8 (6.3)	1.3 (9.2)	2.4 (6.7)	3.3 (9.1)
^{137}Cs	0.050	0.12	0.16	0.30
Net Pb	—	1.5 (8.0)	1.9 (8.4)	4.0 (7.5)
$^{239+240}$Pu	—	—	—	4.0 (7.5)

[a]Based on (2).
[b]Estimated time-integrated atmospheric loadings of excess ^{210}Pb, ^{137}Cs, net Pb, and Pu are 30 dpm cm^{-2}, 15 dpm cm^{-2}, 20μ cm^{-2}, and 0.4 dpm cm^{-2}, respectively. Ratios of ^{137}Cs focusing factors to those of other elements are given in parentheses and expressed in percent.

about 0.2 to 0.8 μg cm^{-2} yr^{-1} in 1978, as compared with a reconstructed mean Pb deposition rate of 0.53 ± 0.02 μg cm^{-2} yr^{-1}. Thus sediment inventories of excess lead are also consistent with a predominantly atmospheric input to Florida Bay.

As of 1995, decay-corrected cumulative atmospheric loading of ^{137}Cs was about 15 dpm cm^{-2}. Inventories of ^{137}Cs are 0.75 ± 0.05, 1.8 ± 0.2, 2.4 ± 0.2, and 4.5 ± 0.3 dpm cm^{-2} (mean ± standard deviation, 2.4 ± 1.6; CV, 65%) at sites 5G, 6A, 6C, and 19C, respectively (Table 5). Thus respective focusing factors are 0.05, 0.12, 0.16, and 0.30 (dpm cm^{-2} sediment/dpm cm^{-2} system). These values are markedly lower than those of other elements. Focusing factor ratios for ^{137}Cs/excess ^{210}Pb are 6.3, 9.2, 6.7, and 9.1%, respectively, and those for ^{137}Cs/excess Pb are 8.0, 8.4, and 7.5% in cores 6A, 6C and 19C, respectively. For core 19C the ^{137}Cs/Pu focusing factor ratio is 7.5%. Thus, relative to other elements, only 8 ± 1% of the ^{137}Cs delivered to the system accumulated at the coring sites. Low inventories of ^{137}Cs, relative to Pu in marine sediments, have been reported by others [*Livingston and Bowen*, 1979; *Olsen et al*., 1981]. This reflects less efficient scavenging of radiocesium in marine systems but not necessarily weaker binding to sediment particles [*Carpenter et al*., 1987; *Santschi et al*., 1983; *Sholkovitz and Mann*, 1984]. Note that the small fraction of ^{137}Cs that is scavenged by particles is codeposited with sediments and the other radioactive and stable elements (Table 5).

4.7. A First-Order System Time-Averaging Model

Temporal records of sediment ^{137}Cs (Figure 9, solid circles) substantially mismatch the fallout record (lightly shaded line). Most of the variability evident in the atmospheric record is absent in all core profiles. Activities decrease more or less exponentially in the postfallout period, between 1970 and dates of core collection (1994–1995). Since the mismatch is not due to in situ dispersive processes such as sediment mixing or radionuclide diffusion, profiles should accurately reflect historical rates of delivery of ^{137}Cs to coring sites. The mismatch can be explained by time averaging atmospheric fluxes of radionuclides and Pb prior to their incorporation into sediments or coral.

Time averaging was proposed by *Benninger and Dodge* [1986] to account for a 30 year record (1951–1980) of fallout plutonium (Pu) in annual growth bands from the coral *M. annularis* at St. Croix, U.S. Virgin Islands. They considered that the peak broadening, as well as the observed 1 year lag between maximum fallout (1963) and maximum Pu in coral (1964), reflected the characteristic time of residence of Pu in a reservoir that they assumed was the well-mixed layer of ocean surface waters. Their "box" model may be written as

$$dF_s/dt = \lambda_s F_a - [\lambda_s + \lambda]F_s, \quad (2)$$

where F_a is the atmospheric flux of Pu, F_s is the flux from the reservoir, $\lambda = \ln 2/t_{1/2}$ (essentially zero for Pu), and $\lambda_s = 1/T_s$, where T_s is the residence time of Pu in the reservoir. Because the relation between Pu in ambient water and in coral layers was not known, Benninger and Dodge took concentrations in annual bands as proportional to F_s. Applying this model, they obtained a value of 2 years for T_s that is comparable to independent estimates of the residence time of Pu in the ocean surface mixed layer. Their model also correctly generated the 1 year lag between the fallout maximum and peak concentration of coral Pu.

Resupply of particle reactive radionuclides and stable elements from well-mixed, presumably sedimentary, "reservoirs" has been invoked by others as well [*Aston and Stanners*, 1981; *Carpenter and Beasley*, 1981; *Koide et al*., 1980; *Livingston and Bowen*, 1979; *Santschi et al*., 1980; *Shen and Boyle*, 1987]. This idea qualitatively explains radionuclide or stable element peak lags, elevated surface concentrations, and backgrounds. The term "reservoir," however, is misleading since it rarely, if ever, refers with certainty to any physical part of a given system. For this reason the more accurate term system time averaging (STA) is employed in this paper. In addition, the STA model

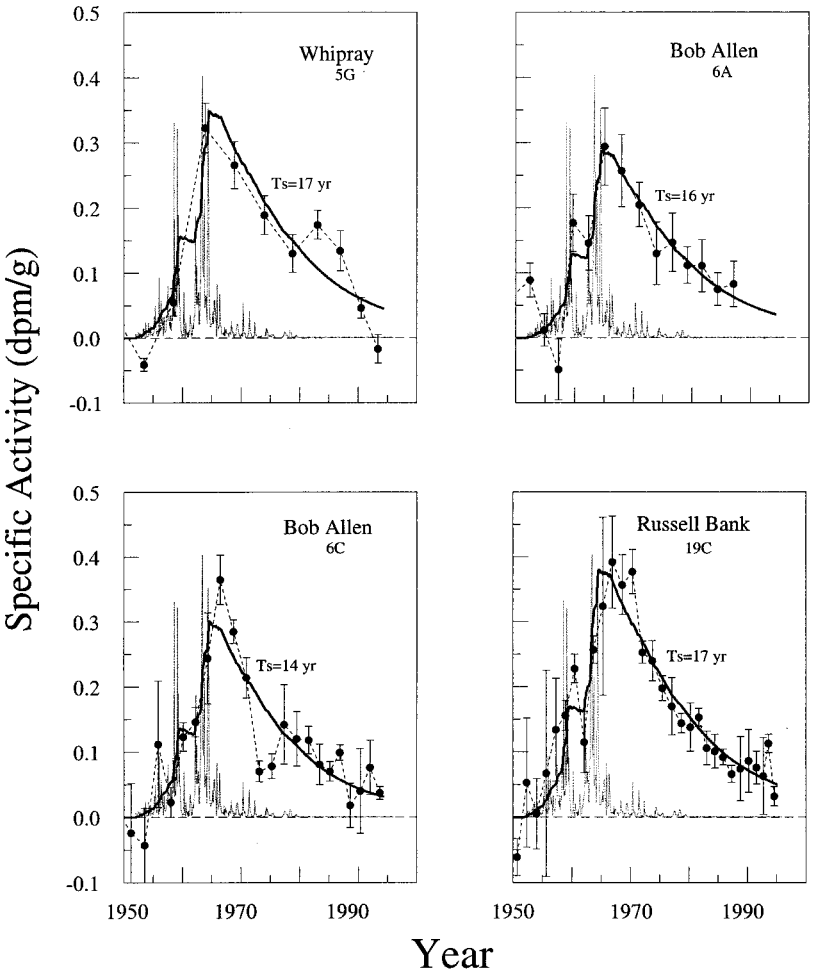

Figure 9. Distributions of ^{137}Cs corrected for radioactive decay. Calculated distributions (heavy solid lines) are based on the system time averaging (STA) model, which subjects atmospheric loads to an unspecified first-order STA process prior to incorporation into sediments and treats ^{137}Cs as immobile thereafter. Age-depth assignments are based on the STA calculation of mean sediment accumulation rates. The ^{137}Cs fallout records (light lines) are superimposed on each plot for comparison. In contrast with 20-fold intrasite variability in $K_d s$ derived from the A-D model, first-order STA time constants T_s are essentially the same at each site, averaging 16 ± 1 years. Shoulders on calculated profiles, associated with the hiatus between major episodes of fallout (1958–1960 and 1962–1965), are also evident in profiles at sites 6A, 6C, and particularly, 19C.

(equation (2)) above describes a specifically first-order time averaging process. In sections 4.7.1 and 4.7.2 this first-order STA model is applied to sedimentary profiles of ^{137}Cs, Pu, and Pb, as well as to the coral Pb record, initially without reference to a specific physical reservoir.

4.7.1. Application to ^{137}Cs and Pu distributions. For trial values of T_s and R_s, distributions were calculated as the solutions to (2), with F_a set equal to monthly ^{137}Cs deposition rates (Figure 2a), and were least squares normalized to ^{137}Cs profiles. This procedure was applied to a large number of trial values in order to select the pair that yielded the global minimum standard deviation in fits. In all cores the STA model provides a better description (Figure 9, solid lines) than the A-D model (compare fit standard deviations in Table 3). Note that the hiatus between two major fallout episodes, 1958–1960 and 1962–1965, produces shoulders in calculated profiles that are apparent in measured profiles at 6A, 6C, and 19C. Sediment accumulation rates, derived from the STA model (Table 3), agree within experimental uncertainties with values based on ^{210}Pb (Table 1) for cores 5G, 6A, and 6C, while for core 19C, values are slightly different, i.e., 1.06 ± 0.04 and 0.92 ± 0.02 g cm^{-2} yr^{-1}. STA model residence times (T_s) range from 14 to 17 years and average 16 ± 1 years. Recently, *Kang* [1999] determined a profile of ^{137}Cs in a core from Jimmie Key located in central Florida Bay about 2 km northwest of Russell Bank site 19C. Application of the STA model to that profile yielded a residence time of 14.1 ± 0.5 years, which accords well with present results. The lag effect noted by *Benninger and Dodge* [1986] is evident in the offset of STA maxima in April 1964 by 1 year from the fallout peak in March 1963 (Figure 9). Note that the 1 year lag in the time-averaged ^{137}Cs flux is sufficiently small that peak dates based on ^{210}Pb are within the experimental errors of the method. The STA model calculation for Pu (19C) includes a 6 year moving average to account for use of composite samples. As a result, the calculated Pu profile (Figure 10) is smoother than model ^{137}Cs profiles (Figure 9). For Pu the STA model residence time is 15.7 ± 0.7 years and mass accumulation rate is 1.03 ± 0.01 g cm^{-2} yr^{-1}. These values are not significantly different from those for ^{137}Cs (Table 3).

4.7.2. Application to coral and sediment lead records. The STA model was applied to net lead profiles in coral and cores using the atmospheric lead concentration record (Figure 2b) as F_a in (2) and optimizing values of T_s. Calculated STA residence times are sensitive to background lead levels in both coral and sediments. Allowing the calculation to choose a background in the case of the coral data resulted in the fit (heavy solid line) shown in Figure 11a for $T_s = 16 \pm 2$ years. The data are shown in terms of total lead with the appropriate amount of background added to the calculated profile. The background of 6 nmol Pb/mol Ca that produces minimum fit variance is somewhat less than the observed background of ~9 nmol Pb/mol Ca, which yields a 24 ± 3 year residence time. The resultant fits to net lead in cores 6A, 6C, and 19C (shown in terms of totals in Figure 11), using a background level of 1.6 ± 0.1 mg kg^{-1}, are satisfactory. However, the STA model underestimates the amount of lead between 1880 and 1920, particularly in core 19C. Derived values of T_s are 15 ± 6, 16 ± 2, and 22 ± 2 years in cores 6A, 6C, and 19C, respectively, average 19 ± 3 years (for 6C and 19C), and are not significantly different from those derived from ^{137}Cs. Because the value of T_s for 6A is very sensitive to uncertainty in R_s owing to a lack of critical data, it has not been included in calculating the average.

For a time constant of 16 years the STA model correctly generates the 6 year lag between the atmospheric lead maximum and peaks in sediment and coral lead records. This lag is illustrated by superimposing the atmospheric lead concentration record on sediment and coral distributions (Figure 11, light solid lines). *Shen and Boyle* [1987] suggested that the lag reflected times for long-range transport of shelf and resuspended lead inputs by anticyclonic currents of the Carribean and North Atlantic Ocean to the Florida Keys. However, the authors noted that because lead is stripped from surface waters in 2–3 years, circulation of mixed surface waters could not produce the observed delay. They concluded that if the lead signal recorded in the Florida Keys coral is due to long-range transport, it must originate from sources involving mixing deeper in the thermocline. The STA analysis provides an alternative explanation for the lag without invoking long-range transport at all.

Note that STA-generated peak lag times depend on temporal characteristics of sources and must not be equated to system residence times. The 6 year peak lag in Pb is in part due to the shoulder beyond the maximum concentration in 1972 (Figure 12a). Such features produce quasi-discontinuous characteristics in lag-residence time relations for Pb and ^{137}Cs (Figure 12b). For Pu the peak lag time jumps to 3 years at a lower residence time ($T_s = 13$ years) than for ^{137}Cs because of the longer half-lives of the plutonium isotopes. First-order STA processes, in principle, do not cause the lags in penetration depths associated with onsets of system loadings. Since there are numerous instances where fallout radionuclide peaks have been used to establish or verify sediment chronologies [*Ritchie and McHenry*, 1990], it is important to consider the potential effects of STA processes on age-depth assignments, and even more so if sediment Pb maxima are used.

The present study suggests that atmospherically delivered ^{210}Pb, like Pb, may be time averaged prior to incorporation into permanent sediments of Florida Bay. With a time constant of 16 years, STA could significantly reduce monthly-to-annual variations in the delivery of excess ^{210}Pb to sediments, thus creating conditions favorable to the use of chronological models, such as (2), which assume a constant rate of supply.

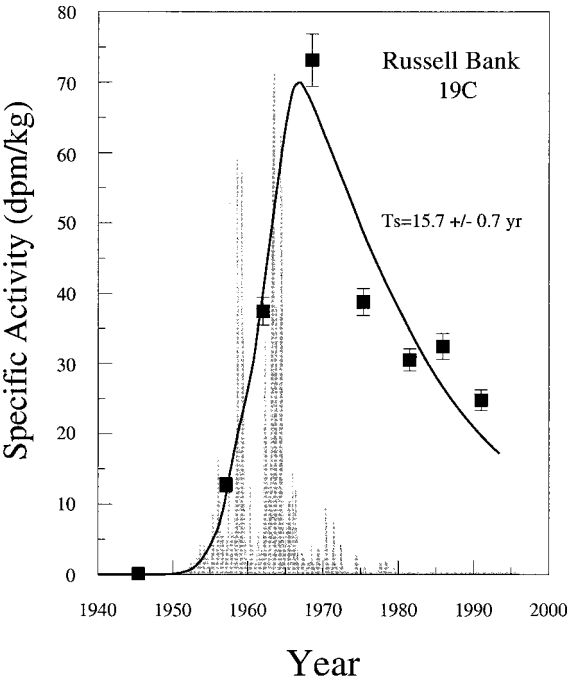

Figure 10. Profile of $^{239+240}$Pu in composite sections of core 19C from Russell Bank. The STA model calculation, which includes a 6 year moving average to account for thick composited core sections, satisfactorily describes the data and yields a residence time of 15.7 ± 0.7 years, which is consistent with results for ^{137}Cs.

4.8. A Proposed STA Process in Florida Bay

It is, of course, uncertain how or where inputs of lead and fallout radionuclides are time averaged en route to permanent deposits in Florida Bay. However, it is reasonable to locate time averaging within the bay itself where mudbanks build through cycles of resuspension, horizontal transport, and redeposition of particles in near-surface sediments largely subject to biological and physical mixing. If so, first-order STA time constants are some appropriately constructed mean times of residence of particles in mixed layers of sediment contributing particles to specific receptor sites. The insensitivity of STA model residence times to differences in loading histories of fallout radionuclides and lead suggests that these tracers have probed the full extent of sediment mixed layers, are insensitive to age-dependent mixing effects [*Smith et al.*, 1993], and have reached steady state with respect to geochemical differences.

In Florida Bay it appears that mixing-free sites such as those selected for the present study may be commingled with areas of mixed sediments on kilometer scales or less. In their core from a site on Bob Allen Bank less than 1 km from sites 6A and 6C, *Rude and Aller* [1991] observed a 20 cm deep near-surface zone of constant ^{210}Pb activity that they attributed either to mixing or to an episode of high deposition. If that layer is a steady state mixing feature, the ratio of its thickness to the sedimentation rate is approximately the particle residence time. For their core this ratio is 20 cm/1.0 cm yr^{-1} = ~20 years, a value compatible with the 16 year residence time of the present study.

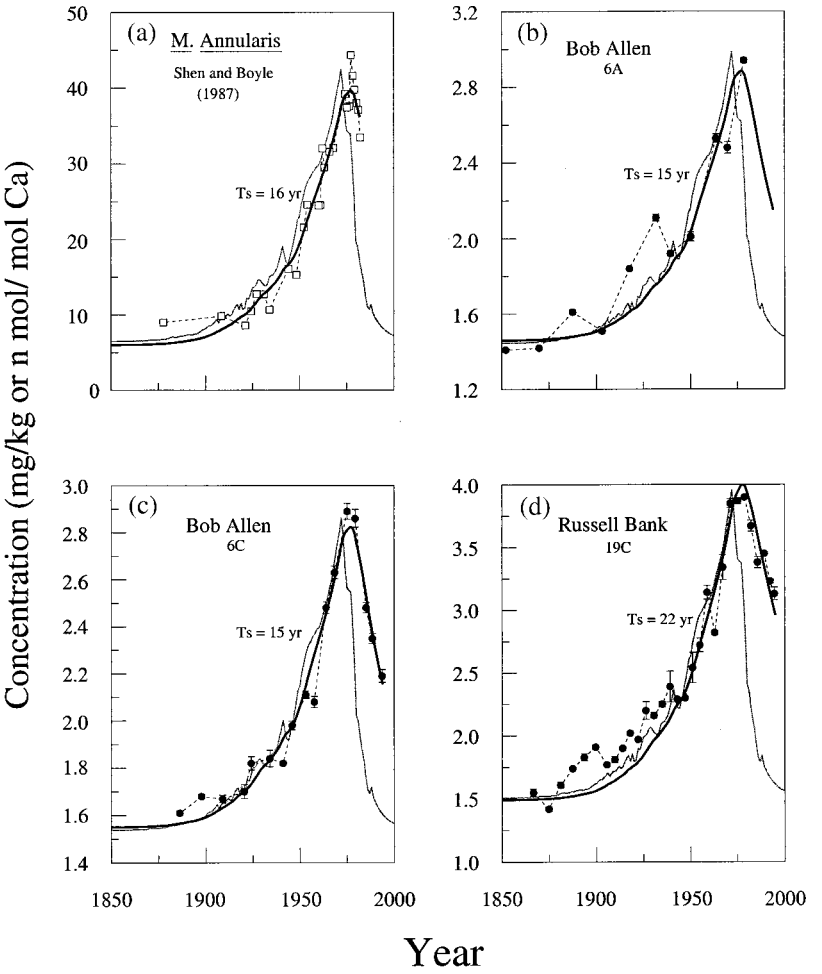

Figure 11. (a) Pb/Ca molar ratio in *M. Annularis* [*Shen and Boyle*, 1987]. Using the lead source function (Figure 2b), the first-order STA model provides a profile (heavy solid line) in excellent accord with the data for a residence time of 16 ± 2 years. The lead source function (light solid line) is shown for comparison. (b), (c), and (d) Profiles of lead versus ^{210}Pb dates. The STA model produces an excellent description of the data, with residence times close to those derived from coral lead, sediment ^{137}Cs, and Pu.

4.9. Commonality of Residence Times?

The consistency of the STA analysis for the coral and spatially resolved sediment receptors does not necessarily mean they received contributions from a common reservoir, nor does it imply that Florida Bay is the primary source of lead in corals on the ocean side of the Keys. In fact, there are several published cases where reanalysis of sediment radionuclide profiles yields STA model time constants of about 10–20 years in marine systems remote from Florida Bay. Reexamination of the Pu record in coral near the Virgin Islands [*Benninger and Dodge*, 1986] reveals that during the postfallout period between 1973 and 1980, Pu concentrations decreased exponentially, yielding a first-order STA time constant of 16 ± 4 years. In cores collected from essentially the same site in Scan Bay, Alaska, in 1980, 1984, 1987, and 1990 by *Sugai et al*. [1994] the STA approach produced excellent representations of the data and yielded residence times of 10.8, 13.7, 13.5, and 14.0 years, respectively. Application of the STA model to $^{239+240}$Pu and ^{238}Pu ($t_{1/2}$ = 88 years) profiles in a ^{210}Pb-dated core (G) collected by *Carpenter and Beasley* [1981] from Saanich Inlet, near Victoria, British Columbia, produced reasonable profiles and yielded residence times of 13.5 and 13.2 years, respectively. Also, the STA model at least partly accounted for the previously unexplained colocation of sediment $^{239+240}$Pu and ^{238}Pu peaks, although maximum ^{238}Pu fallout from SNAP-9A device burnup occurred 3–5 years later than Pu.

A significant commonality of STA residence times, around 10–20 years as this somewhat limited selection of examples suggests, would seem to result from physical or biogeochemical conditions that tend to preserve the ratio of mixed layer depth to sediment accumulation rate in at least some coastal marine environments. Furthermore, decade-scale residence times could be an "artifact" of selecting coastal environments where ^{210}Pb is a primary chronometer. This curious result may be a corollary of *Boudreau*'s [1994] finding that radionuclide-determined mixed depths in marine sediments are surprisingly independent of sedimentation rates, an observation later argued to be a consequence of the coupling between bioturbation rates and sediment nutrient content [*Boudreau*, 1998]. The worldwide average is 10 ± 5 cm for 203 reported observations in which rates varied by five orders of magnitude. Since the ^{210}Pb method is generally used in situations where rates range from about 0.2 to 5 cm yr^{-1}, sediments dominated by bioturbated deposits, where this method is successfully applied, will yield mixed layer residence times between 2 and 50 years.

In a seemingly unrelated observation a nearly exponential

decline in Pb concentrations, between 1983 and 1996 in surface waters of the Sargasso Sea near Bermuda [*Wu and Boyle*, 1997], is also characterized by a 16 ± 1 year time constant (using (2) with $F_a = 0$). It drops to 13 years if F_a is set equal to the atmospheric Pb concentration (Figure 2b). Perhaps reservoirs of mixed coastal sediments contribute Pb to the surface mixed layer of the Sargasso Sea through resuspension and horizontal transport. Such a mechanism could not only explain the calculated decade-scale time constant but would predict further declines in surface waters in the absence of other sources of Pb. In contrast, *Wu and Boyle* [1997] suggested that atmospheric emissions from high-temperature industrial processes in the United States are presently maintaining Pb loading at levels that will support future concentrations in surface water close to those measured in 1996. If decade-scale residence times are a widely occurring property of coastal marine sedimentary environments, then perhaps observations of decade-scale declines in concentrations of key tracers in noncoastal pelagic regions of the ocean might constitute prima facie evidence for cross-margin transport of materials from coastal sources.

5. Summary

This study shows that chronologies of recent undisturbed sediments from the mudbanks in central Florida Bay can be established by measuring vertical distributions of ^{210}Pb and ^{226}Ra in X radiographically evaluated cores from carefully selected sites. Chronologies spanning the preceding 70–90 years were confirmed by excellent agreement between temporal records of stable Pb in ^{210}Pb-dated sediments and Pb/Ca ratios in annual layers of coral (*M. annularis*) located on the ocean side of the Florida Keys [*Shen and Boyle*, 1987]. The sediment core data support *Shen and Boyle*'s [1987] observation of a 6 year lag between peak atmospheric Pb concentrations (1972) and maximum Pb in coral (1978). Comparability of excess Pb/excess ^{210}Pb ratios in sediment and coral layers of the same age, and in rain [*Settle et al*., 1982], suggest that the atmosphere is the primary source of lead species (both Pb and ^{210}Pb) delivered to sediments and coral. Both receptors evidently accumulate lead species in proportion to concentrations in ambient waters despite differences in principal modes of incorporation: particle scavenging versus coral lattice binding of dissolved Pb.

Depths of penetration and maximum activity of ^{137}Cs and Pu in sediments are correctly given by ^{210}Pb/^{226}Ra dating as well. Apart from this agreement, however, profiles bear little resemblance to a 30 year record of highly variable monthly rates of ^{137}Cs fallout in the region. Deposition peaked in the mid-1960s with negligible additional inputs after the mid-1970s. In contrast, activities of Pu and decay-corrected ^{137}Cs in cores have decreased more or less exponentially since the mid-1970s and remain significantly above background more than 20 years later. The persistence of fallout activity in sediments cannot be explained by interstitial migration of radiocesium and plutonium, as illustrated by application of a conventional advection-diffusion (A-D) model with local equilibrium and reversible isotopic exchange. The immobility of radiocesium in sediments of Florida Bay is further supported by comparison of vertically integrated activities or concentrations of excess ^{210}Pb, excess Pb, ^{137}Cs, and Pu. All four elements have accumulated in proportion to rates of sediment accumulation among sites and are probably moving with particles in the bay. However, only 8% of atmospherically delivered radiocesium reached sediments compared with excess ^{210}Pb, excess Pb, and Pu.

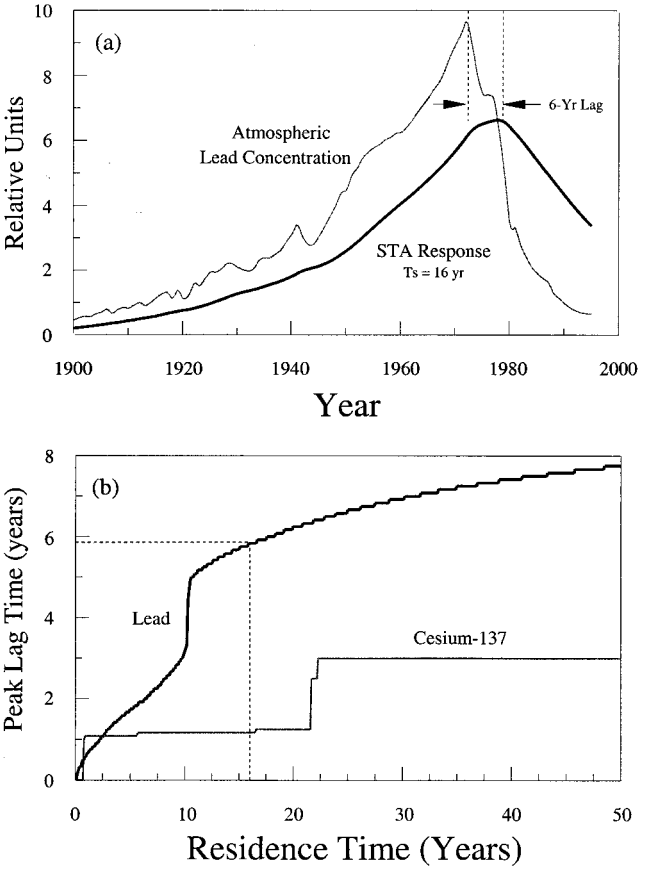

Figure 12. (a) Effect of first-order STA on the lead flux for a residence time of 16 years. In addition to peak lags, temporal variations in the input are lost in the coral record, as noted by *Shen and Boyle* [1987], and in sediments as well. (b) Peak lag time versus residence time for lead and cesium-137. Quasi-discontinuous features are produced by contributions from small structures on declining sides of principal maxima. A residence time of 16 years (vertical dashed line) situates peak lag times within stable regions of lag-residence time relations. The observed 6 year lag between the atmospheric maximum (1972) and peak values in coral and sediments (1978) is correctly given by the first-order STA model (horizontal dashed line). While residence times are largely system properties, peak lag times depend strongly on source function characteristics.

Distributions of lead and radionuclides are explained by a first-order system time averaging (STA) in which such elements, attached to particles, are mixed in a reservoir of unspecified location with a characteristic (residence) time before resupply to sediments or coral. The STA model yields remarkably consistent estimates of particle residence times independent of element, loading history, or archiving medium: for sediment ^{137}Cs, 16 ± 1 ($n = 4$); for Pu, 15.7 ± 0.7 ($n = 1$); for Pb, 19 ± 3 ($n = 2$); and for coral Pb, 16 ± 2 years ($n = 1$). The model generates the 6 year, atmosphere-sediment/coral peak lags without invoking long-range transport of lead by ocean currents [*Shen and Boyle*, 1987]. Present results suggest that areas of unmixed sediments in Florida Bay are commingled with and receive particles resuspended from reservoirs of physically and biologically mixed near surface deposits. The 16 year mean reservoir residence time ensures that significant

levels of particle-associated nondegradable contaminants like lead will persist for decades following cessation of loads to Florida Bay and the coastal ocean near the Keys. An analysis of selected sediment radionuclide profiles reported by others, suggests that decade-scale time averaging may be a general feature of coastal marine sedimentary environments.

Acknowledgments. We express our appreciation to N. Morehead, Great Lakes Environmental Research Laboratory, and M. Marot, U.S. Geological Survey, St. Petersburg, for their help in sample collection, sample preparation, and radioanalytical measurement; R. Rood, Cooperative Institute for Limnology and Ecosystems Research, University of Michigan, for assistance in radioanalytical measurement and manuscript preparation; and T. Dvonch, School of Public Health, University of Michigan, for assistance in ICP-MS measurement. The X radiographs were provided by the Fishermen's Hospital in Marathon, Florida, when we worked in the southern bay and by the Mariners Hospital on Plantation Key when we worked in the upper bay. We are grateful to L. Benninger, G. Brunskill, E. Callender, and D. N. Edgington for their helpful comments. Contribution 1069 of the Great Lakes Environmental Research Laboratory.

References

Appleby, P. G., and F. Oldfield, Application of ^{210}Pb to sedimentation studies, in *Uranium-Series Disequilibrium: Applications to Earth, Marine and Environmental Sciences*, 2nd ed., edited by M. Ivanovich and R. S. Harmon, pp. 731–778, Clarendon, Oxford, England, 1992.

Armentano, T., J. Hunt, D. Rudnick, N. Thompson, P. Ortner, M. Robblee, and R. Halley, Strategic plan for the Interagency Florida Bay Science Program, report, Florida Bay Program Manage. Comm., Everglades National Park, 1997.

Aston, S. R., and D. A. Stanners, Plutonium transport to and deposition and immobility in Irish Sea intertidal sediments, *Nature*, *289*, 581–582, 1981.

Bahr, J. M., and J. Rubin, Direct comparison of kinetic and local equilibrium formulations for solute transport affected by surface reactions, *Water Resources Res*., *23*, 438–452, 1987.

Ball, M. M., E. A. Shinn, and K. W. Stockman, The geologic effects of Hurricane Donna in south Florida, *J. Geol*., *75*, 583–597, 1967.

Benninger, L. K., and R. E. Dodge, Fallout plutonium and natural radionuclides in annual bands of the coral *Montastrea annularis*, St. Croix, U.S. Virgin Islands, *Geochim. Cosmochim. Acta*, *50*, 2785–2797, 1986.

Berner, R. A., *Early Diagenesis: A Theoretical Approach*, Princeton Univ. Press, Princeton, N. J., 1980.

Boscence, D. W. J., Biogenic carbonate production in Florida Bay, *Bull. Mar. Sci*., *44*, 419–433, 1989a.

Boscence, D. W. J., Surface sublittoral sediments of Florida Bay, *Bull. Mar. Sci*., *44*, 434–453, 1989b.

Boscence, D. W. J., Anatomy of a recent biodetrital mud-mound, Florida Bay, USA, *Spec. Publ. Int. Assoc. Sedimentol*., *23*, 475–493, 1995.

Boudreau, B. P., Is burial velocity a master parameter for bioturbation?, *Geochim. Cosmochim. Acta*, *58*, 1243–1249, 1994.

Boudreau, B. P., Mean mixed depth of sediments: The wherefore and the why, *Limnol. Oceanogr*., *43*, 524–526, 1998.

Carlson, P. R., L. A. Yarbro, and T. R. Barber, Relationship of sediment sulfide to mortality of *Thalassia testudinum* in Florida Bay, *Bull. Mar. Sci*., *54*, 733–746, 1994.

Carpenter, R., and T. M. Beasley, Plutonium and americium in anoxic marine sediments: Evidence against remobilization, *Geochim. Cosmochim. Acta*, *45*, 1917–1930, 1981.

Carpenter, R., T. M. Beasley, D. Zahnle, and B. L. K. Somayajulu, Cycling of fallout (Pu, ^{241}Am, ^{137}Cs) and natural (U, Th, ^{210}Pb) radionuclides in Washington continental slope sediments, *Geochim. Cosmochim. Acta*, *51*, 1897–1921, 1987.

Carter, M. W., and A. A. Moghissi, Three decades of nuclear testing, *Health Phys*., *33*, 55–71, 1977.

Comans, R. J. N., and D. E. Hockley, Kinetics of cesium sorption on illite, *Geochim. Cosmochim. Acta*, *56*, 1157–1164, 1992.

Culotta, E., Bringing back the Everglades, *Science*, *268*, 1688–1690, 1995.

Cutshall, N. H., I. L. Larsen, and C. R. Olsen, Direct analysis of ^{210}Pb in sediment samples: Self-absorption corrections, *Nucl. Instrum. Methods Phys. Res*., *26*, 309–312, 1983.

Davies, T. D., and A. D. Cohen, Composition and significance of the peat deposits of Florida Bay, *Bull. Mar. Sci*., *44*, 387–398, 1989.

Drafting Committee, Science plan for Florida Bay, report, Everglades National Park, 1994.

Eisenreich, S. J., N. A. Metzer, N. R. Urban, and J. A. Robbins, Response of atmospheric lead to decreased use of lead in gasoline, *Environ. Sci. Technol*., *20*, 171–174, 1986.

Enos, P., Islands in the bay: A key habitat of Florida Bay, *Bull. Mar. Sci*., *44*, 365–386, 1989.

Enos, P., and R. D. Perkins, Evolution of Florida Bay from island stratigraphy, *Bull. Geol. Soc. Am*., *90*, 59–83, 1979.

Fleece, J. B., The carbonate geochemistry and sedimentology of the Keys of Florida Bay, Florida, *Contrib. 5*, Sediment. Res. Lab., Dep. of Geol., Fla. State Univ., Tallahassee, 1962.

Flynn, W. W., The determination of ^{210}Po in environmental materials, *Anal. Chim. Acta*, *43*, 121–131, 1968.

Ginsburg, R. N., Constituent particles in some south Florida carbonate sediments, *Bull. Am. Assoc. Petrol. Geol*., *40*, 2384–2427, 1956.

Ginsburg, R. N., and R. M. Lloyd, A manual piston coring device for use in shallow water, *J. Sed. Petrol*., *26*, 64–66, 1956.

Goldberg, E. D., Geochronology with ^{210}Pb, in *Radioactive Dating*, pp. 121–122, Int. At. Energy Agency, Vienna, Austria, 1963.

Graney, J. R., A. N. Halliday, G. J. Keeler, J. O. Nriagu, J. A. Robbins, and S. A. Norton, Isotopic record of lead pollution in lake sediments from the northeastern United States, *Geochim. Cosmochim. Acta*, *59*, 1715–1728, 1995.

Health and Safety Laboratory (HASL), Final tabulation of monthly ^{90}Sr fallout data: 1954–1976, *Rep. HASL-329*, U.S. Energy Res. and Dev. Admin., Washington, D. C., 1977.

Holloway, M., Nurturing nature, *Sci. Am*., *270*, 98–108, 1994.

Holmes C., J. A. Robbins, R. Halley, M. Bothner, M. tenBrink, M. Marot, E. Shinn, and D. Rudnick, Retrospective analysis of Florida Bay sediments, in *Final Report to the South Florida Water Management District*, contract C-E7606, West Palm Beach, Fla., 1998.

Kang, W.-J., Inputs of sediment and mercury to the lower Everglades and Florida Bay: A temporal and spatial perspective, Ph.D. thesis, 129 pp., Div. of Mar. and Environ. Syst., Fla. Inst. of Technol., Melbourne, 1999.

Kaplan, D. I., P. M. Bertsch, D. C. Adriano, and K. A. Orlandini, Actinide association with groundwater colloids in a coastal plain aquifer, *Radiochim. Acta*, *66/67*, 181–187, 1994.

Koide, M., E. D. Goldberg, and V. Hodge, ^{241}Pu and ^{241}Am in sediments from coastal basins off California and Mexico, *Earth Planet. Sci. Lett*., *48*, 250–256, 1980.

Koide, M., R. Michel, E. D. Goldberg, M. M. Herron, and C. C. Langway Jr., Characterization of pre- and post-moratorium tests to polar ice caps, *Nature*, *296*, 544–547, 1982.

Krey, P. W., E. P. Hardy, C. Pachucki, F. Rourke, J. Coluzza, and W. K. Benson, Mass isotopic composition of global fall-out plutonium in soil, in *Transuranic Nuclides in the Environment*, *IAEA-SM-199/39*, pp. 671–676, Int. At. Energy Agency, Vienna, 1976.

Livingston, H. D., and V. T. Bowen, Pu and ^{137}Cs in coastal waters, *Earth Planet. Sci. Lett*., *43*, 29–45, 1979.

Manker, J. P., and G. M. Griffin, Source and mixing of insoluble clay minerals in a shallow water carbonate environment-Florida Bay, *J. Sediment. Petrol*., *41*, 302–306, 1971.

Nriagu, J. O., The rise and fall of leaded gasoline, *Sci. Total Environ*., *92*, 13–28, 1990.

Olsen, C. R., H. J. Simpson, and R. M. Trier, Plutonium, radiocesium and radiocobalt in sediments of the Hudson River estuary, *Earth Planet. Sci. Lett*., *55*, 377–392, 1981.

Press, W. H., B. P. Flannery, S. A. Teukolsky, and V. T. Vetterling, *Numerical Recipes: The Art of Scientific Computing*, Cambridge Univ. Press, New York, 1989.

Ritchie, J. C., and J. R. McHenry, Application of radioactive fallout ^{137}Cs for measuring soil erosion and sediment accumulation rates and patterns: A review, *J. Environ. Qual*., *19*, 215–233, 1990.

Robbins, J. A., Geochemical and geophysical applications of radioactive lead, in *Biogeochemistry of Lead in the Environment*, vol. 1A, edited by J. O. Nriagu, pp. 285–393, Elsevier Sci., New York, 1978.

Robbins, J. A., Great Lakes regional fallout source functions, *Tech. Memo. ERL-GLERL-56*, 21 pp., Great Lakes Environ. Res. Lab., Ann Arbor, Mich., 1985.

Robbins, J. A., A model for particle-selective transport of tracers in sediments with conveyor belt deposit feeders, *J. Geophys. Res*., *91*, 8542–8558, 1986.

Robbins, J. A., and L. R. Herche, Models and uncertainty in ^{210}Pb dating of sediments, *Verh. Int. Ver. Limnol*., *25*, 217–222, 1993.

Roblee, M. B., T. R. Barber, P. R. Carlson, M. J. Durako, J. W. Fourqurean, L. K. Muehlstein, D. Porter, L. A. Yarbro, R. T. Zieman, and J. C. Zieman, Mass mortality of the tropical seagrass, Thalassia testudinum, in Florida Bay, *Mar. Ecol. Proc. Ser*., *71*, 297–299, 1991.

Rude, P. D., and R. C. Aller, Fluorine mobility during early diagenesis of carbonate sediment: An indicator of mineral transformation, *Geochim. Cosmochim. Acta*, *55*, 2491–2509, 1991.

Santschi, P. H., Y. H. Li, J. J. Bell, R. M. Trier, and K. Kawtaluk, Pu in coastal marine environments, *Earth Planet. Sci. Lett*., *51*, 248–265, 1980.

Santschi, P. H., Y. H. Li, D. M. Adler, M. Amdurer, J. Bell, and U. P. Nyffeler, The relative mobility of natural (Th, Pb and Po) and fallout (Pu, Am, Cs) radionuclides in the coastal marine environment: Results from model ecosystems (MERL) and Naragansett Bay, *Geochim. Cosmochim. Acta*, *47*, 201–210, 1983.

Scholl, D. W., Recent sedimentary record in mangrove swamps and rise in sea level over the southwestern coast of Florida, part I, *Mar. Geol*., *1*, 344–366, 1964a.

Scholl, D. W., Recent sedimentary record in mangrove swamps and rise in sea level over the southwestern coast of Florida, part II, *Mar. Geol*., *2*, 343–364, 1964b.

Scholl, D. W., F. W. Craighead Sr., and M. Stuiver, Florida submergence curve revised: Its relation to sedimentation rates, *Science*, *163*, 562–564, 1969.

Science Sub-Group, South Florida ecosystem restoration: Scientific information needs, report, Everglades National Park, Fla., 1995.

Settle, D. M., C. C. Patterson, K. K. Turekian, and J. K. Cochran, Lead precipitation fluxes at tropical oceanic sites determined from ^{210}Pb measurements, *J. Geophys. Res*., *87*, 1239–1245, 1982.

Shen, G. T., and E. A. Boyle, Lead in corals: Reconstruction of historical industrial fluxes to the surface ocean, *Earth Planet. Sci. Lett*., *82*, 289–304, 1987.

Shen, G. T., and E. A. Boyle, Determination of lead, cadmium and other trace metals in annually-banded corals, *Chem. Geol*., *67*, 47–62, 1988.

Sholkovitz, E. R., The geochemistry of plutonium in fresh and marine water environments, *Earth Sci. Rev*., *19*, 95–161, 1983.

Sholkovitz, E. R., and D. R. Mann, The pore water chemistry of Pu and ^{137}Cs in sediments of Buzzards Bay, Massachusetts, *Geochim. Cosmochim. Acta*, *48*, 1107–1114, 1984.

Sholokvitz, E. R., J. K. Cochran, and A. E. Carey, Laboratory studies of the diagenesis and mobility of Pu and ^{137}Cs in nearshore sediments, *Geochim. Cosmochim. Acta*, *47*, 1369–1379, 1983.

Smith, C. R., R. H. Pope, D. J. DeMaster, and L. Magaard, Age-dependent mixing of deep-sea sediments, *Geochim. Cosmochim. Acta*, *57*, 1473–1488, 1993.

Stehli, F. G., and J. Hower, Mineralogy and early diagenesis of carbonate sediments, *J. Sediment. Petrol*., *31*, 358–371, 1961.

Stockman, K. W., R. N. Ginsburg, and E. A. Shinn, The production of lime mud by algae in south Florida, *J. Sediment. Petrol*., *37*, 633–648, 1967.

Sugai, S. F., M. J. Alpern, and W. S. Reeburgh, Episodic deposition and ^{137}Cs immobility in Skan Bay sediments: A ten-year ^{210}Pb and ^{137}Cs time series, *Mar. Geol*., *116*, 351–372, 1994.

Taft, W. H., and J. W. Harbaugh, Modern carbonate sediments of Southern Florida, Bahamas, and Espiritu Santo Island, Baja, California: A comparison of their mineralogy and chemistry, *Stanford Univ. Publ. Geol. Sci*., *8*, 133 pp., 1964.

Thayer, G. W., P. L. Murphey, and M. W. Lacroix, Responses of plant communities in western Florida Bay to the die-off of sea grasses, *Bull. Mar. Sci*., *54*, 718–726, 1994.

Urban, N. R., S. J. Eisenreich, D. F. Grigal, and K. T. Schurr, Mobility and diagenesis of Pb and ^{210}Pb in peat, *Geochim. Cosmochim. Acta*, *54*, 3329–3346, 1990.

Wanless, H. R., and M. G. Tagett, Origin, growth and evolution of carbonate mudbanks in Florida Bay, *Bull. Mar. Sci*., *44*, 454–489, 1989.

Wu, J., and E. A. Boyle, Lead in the western North Atlantic Ocean: Completed response to leaded gasoline phaseout, *Geochim. Cosmochim. Acta*, *61*, 3279–3283, 1997.

M. Bothner and M. tenBrink, Marine and Coastal Program, Woods Hole Field Center, U.S. Geological Survey, 384 Woods Hole Road, Woods Hole, MA 02543.

J. Graney and G. Keeler, School of Public Health, Department of Environmental and Industrial Health, University of Michigan, Ann Arbor, MI 48109.

R. Halley, C. Holmes, and E. Shinn, Center for Coastal and Regional Marine Geology, U.S. Geological Survey, 600 4th Street S., St. Petersburg, FL 33701.

K. A. Orlandini, Environmental Research Division, Argonne National Laboratory, 9700 S. Cass Avenue, Argonne, IL 60439.

J. A. Robbins, Great Lakes Environmental Research Laboratory, NOAA, U.S. Department of Commerce, 2205 Commonwealth Boulevard, Ann Arbor, MI 48105. (robbins@glerl.noaa.gov)

D. Rudnick, South Florida Water Management District, 3301 Gun Club Road, West Palm Beach, FL 33146.

(Received August 6, 1998; revised November 10, 1999;
accepted June 13, 2000.)